Desalination and Water Treatment
www.deswater.com

doi: 10.1080/19443994.2013.789405

52 (2014) 1589–1599
February

Taylor & Francis
Taylor & Francis Group

Adsorption of Reactive Blue 21 from aqueous solutions onto clay, activated clay, and modified clay

Ageetha Vanaamudan, Naznin Pathan, Padmaja Pamidimukkala*

Faculty of Science, Department of Chemistry, The M.S. University of Baroda, Sayjigunj, Vadodara 390002, India
Tel. +91 265 2795552; Fax: +91 265 2795552; email: p_padmaja2001@yahoo.com

Received 25 December 2012; Accepted 15 March 2013

ABSTRACT

The objectives of this work were to investigate the adsorption of Reactive Blue 21(RB21) onto clay(C), activated clay (AC), and modified clay (MC). The adsorbents were characterized by FTIR, XRD, TGA, and BET. Batch studies were carried out to evaluate parameters affecting adsorption such as contact time, pH, sorbent dose, and temperature. Among the kinetic models tested, the adsorption kinetics was best described by the pseudo-second-order equation. The data fitted well with Freundlich, Langmuir, Temkin, and Halsey isotherms. The reusability of the adsorbents using 1 N NaOH for over three cycles indicates the economic significance of these materials as adsorbents.

Keywords: Activated clay; Adsorption; Clay; Modified clay; Reactive Blue

1. Introduction

Effluents from the textile industry contain various kinds of synthetic dyestuffs, and there has been increased interest in decolorization of these effluents in the last few decades. Basic and reactive dyes are extensively used in the textile industry because of their favorable characteristics of bright color, solubility in water, simple application technique, and low-energy consumption [1]. Dye effluents are not only esthetic pollutants because of their color but also interfere with light penetration into water bodies, thereby disturbing the biological processes. Further, dye effluents contain chemicals that are toxic toward microbial populations and are carcinogenic to mammals. Therefore, environmental legislation had imposed stringent limits on the concentrations of pollutants that are discharged in aqueous effluents from dyestuff manufacturing and textile industries. Among the methods of effluent treatment, adsorption technology was generally considered to be an effective method for removal of dyes [2–4]. Aluminosilicates such as zeolites, bentonite, and montmorillonite have been recognized as promising low-cost adsorbents for environmental applications [5–11]. Montmorillonite (Mt) is widely used as an adsorbent due to its high specific surface area, chemical and mechanical stabilities, and a variety of surface and structural properties [12–16]. In order to improve the adsorption properties of Mt, it has been activated with acid and modified with surfactants. Acid treatment generally increases the surface area and acidity of the clay (C) [17]. Substitution of interlayer cations of clay with cationic surfactants [18–22] is the basic requirement for making Mt suitable for removal of anionic species such as reactive dyes and oxyanions from wastewater [22–26]. In this study Mt (C), acid activated Mt (AC)

*Corresponding author.

and surfactant modified Mt (MC) were characterized and compared for their ability to adsorb Reactive Blue (RB21) from aqueous solution.

2. Materials and methods

Commercial grade Reactive blue dye was used without further purification. Montmorillonite (C) and Cetyltrimethylammonium bromide (CTAB) were purchased from Sigma Aldrich.

2.1. Acid activation of clay

Acid activation of the clays was carried out by treating with 0.25 M H_2SO_4. Twenty grams of Mt was refluxed with 200 ml of 0.25 M H_2SO_4 for 180 min. The activated clay (AC) was centrifuged and washed with water several times, till it was free of SO_4^{2-} and dried at 373 K in an air oven until constant mass was attained [27].

2.2. Modification of clay

Surfactant (CTAB) equivalent to (0.2473 × CEC of clay) was dissolved in 100 ml distilled water. A total of 5 g of clay was added to the surfactant solutions and stirred for 12 h at 60˚C. The surfactant modified Mt modified clay (MC) was separated by centrifugation and washed with water for the removal of bromide. It was then dried in vacuum for three days [28].

2.3. Preparation of dye solutions

Stock solutions of RB21 (1 g/L) were prepared by dissolving accurately weighed amount of RB21 in double-distilled water and subsequently diluting to the required concentration. The structure of the dye is shown in Fig. 1.

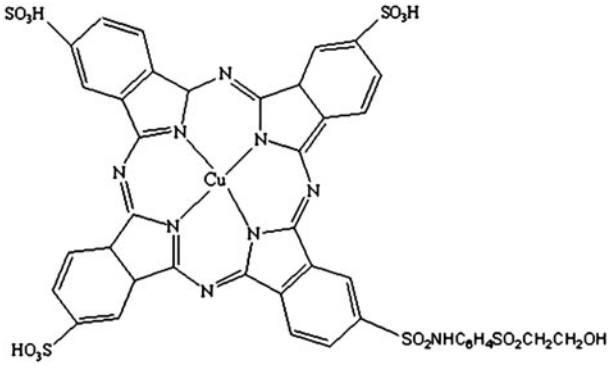

Fig. 1. Structure of Reactive Blue 21.

2.4. Batch sorption experiments

Experiments were conducted to study the effect of various parameters for the removal of Reactive Blue 21 (RB21) on natural clay (C), AC, and MC. For each experiment, 25 mL of dye solutions of known initial concentrations and pH was taken in 100-mL stoppered conical flasks. A suitable adsorbent dose is added to the solution and the mixture was agitated at a constant speed. The supernatant was separated from the adsorbent by filtration and analyzed for the presence of unadsorbed dye by using SYSTRONICS Digital 166 model visible spectrophotometer. The percentage removal of the dye and the amount adsorbed (mg/g) were calculated by the following relationship:

$$q_e = \frac{(C_i - C_e)}{m} \quad (1)$$

where C_i—initial concentration of dye in mg/L; C_e—equilibrium concentration of dye in mg/L; m—mass of adsorbent g/L; q_e—amount of dye adsorbed per gram of adsorbent.

2.5. Statistical analysis

In order to ensure the reproducibility of results, experiments were replicated three times and data presented were the mean values from these independent experiments. Experimental errors were estimated, and standard deviations are indicated wherever necessary.

2.6. Equilibrium sorption studies

Adsorption isotherms were determined by the treatment of 0.05 g of adsorbent under study with dye solution having an initial concentration varying from 100 to 1,000 mg/L in a thermostated rotary mechanical shaker. After agitation, the contents of the flasks were filtered. The concentration of dye remaining in the solution was determined by spectrophotometer. The results of experimental measurements were in the form of adsorption isotherms. Attempts were made to fit the equilibrium dye sorption isotherm data to a number of well-known models (Table 1) such as Freundlich, Langmuir, Temkin, Flory-Huggins, and Halsey for the better understanding of the processes governing adsorption of dye on to the adsorbents under study. The results are shown in Table 2.

2.7. Sorption dynamics

In order to investigate the sorption process of the dye pseudo first order, pseudo second order, intraparticle

Table 1
Isotherm and kinetic models

Eq^n	Isotherm	Functional form	Plotting
I	Freundlich	$q_e = K_f C_e^{1/n}$	$\text{Log}\, q_e$ vs. $\text{Log}\, C_e$
II	Langmuir	$\frac{q_e}{q_m} = \frac{K_L C_e}{1+K_L C_e}$	$\frac{1}{q_e}$ vs. $\frac{1}{C_e}$
III	Temkin	$\frac{q_e}{q_m} = \frac{R_T}{\Delta Q}\text{Ln}(K_T C_e)$	q_e vs. $\text{Ln}C_e$
IV	Flory–Huggins	$\text{Log}\frac{\theta}{C_0} = \text{Log}K_{FH} + \eta_{FH}\text{Log}(1-\theta)$	$\text{Log}\frac{\theta}{C_0}$ vs. $\text{Log}(1-\theta)$
V	Halsey	$q_e = K_H/C_e^{1/(\eta)H}$	$\text{Log}.q_e$ vs. $\text{Log}\, C_e$
VI	Dubinin–Radushkevich	$\frac{q_e}{q_m} = \exp(-\beta\varepsilon^2)$ with $\beta = \frac{1}{E^2}$ and $\varepsilon = RT\text{Ln}\frac{C_s}{C_e}$	$\text{Ln}\, q_e$ vs. $\left(\text{Ln}(\frac{C_s}{C_e})\right)^2$
Kinetics			
I	Pseudo 1st order	$\frac{dq}{dt} = K_i'(q_e - q_t)$	$\text{Log}(q_e - q_t)$ vs. t
II	Pseudo 2nd order	$\frac{q_e^2 K_i'}{1+q_e K t}$	$\frac{t}{qt}$ vs. t
III	Intraparticle diffusion	$q_t = K_i t^{0.5}$	q_t vs. $t^{0.5}$
IV	Bangham	$\text{Log}\,\text{Log}\left(\frac{C_0}{C_0 - q_t m}\right) = \text{Log}\left(\frac{K_m}{2.303V} + \propto \text{Log}\ t\right)$	$\text{Log}\,\text{Log}\left(\frac{C_0}{C_0 - q_t m}\right)$ vs. L
V	Liquid Film diffusion	$\text{Ln}\left(1 - \frac{q_t}{q_e}\right) = -K_{FD}t$	$\text{Ln}\left(1 - \frac{q_t}{q_e}\right)$ vs. t

diffusion, Bangham, and liquid film diffusion models were used as kinetic models (Table 1). The values of correlation coefficients and standard deviation were used to compare the models which are shown in (Table 3). SD was calculated using the equation.

$$\text{SD} = \sqrt{\frac{1}{N}\sum_{i=1}^{N}(x_i - \bar{x})^2} \tag{2}$$

2.8. Thermodynamics of sorption studies

The thermodynamic parameters of the adsorption process could be determined from the experimental data obtained at various temperatures using the equations:

$$K_d = \frac{q_e}{C_e} \tag{3}$$

$$\ln K_d = \frac{\Delta S^0}{R} - \frac{\Delta H^0}{RT} \tag{4}$$

$$\Delta G^0 = \Delta H^0 - T\Delta S^0 \tag{5}$$

2.9. Fourier transform infrared spectroscopy

FTIR was used to determine the changes in vibrational frequencies of the functional groups in the adsorbents. The spectra were collected by a Perkin Elmer RX1 model within the wave number range of 400–4,000 cm^{-1}. Specimens of samples were first mixed with KBr and then ground in an agate mortar at an appropriate ratio of 1/100 for the preparation of the pellets. Resulting mixture was pressed at 10 tons for 5 min. Sixteen scans and 8 cm^{-1} resolution were applied in recording spectra. The background obtained from the scan of pure KBr was automatically subtracted from the sample spectra.

2.10. Thermogravimetric analysis

Thermogravimetric analysis was done using EXSTAR6000 TG/DTA 6300 model instrument. The measurements were carried out under a nitrogen atmosphere. Samples weighing in the range of 5–10 mg were taken in the sample pan, and the temperature was raised from 30−600 °C at a heating rate of 10 °C per minute. The mass of the sample pan was continuously recorded as a function of temperature.

2.11. X-ray diffraction studies of clay, activated clay, and modified clay

X-ray diffraction patterns were measured by a Rigaku ultima-3 instrument. Powder XRD of the samples was taken by holding the sample in place on quartz plate for exposure to Cu Kα radiation of wavelength 1.54184 Å with the two-theta scanning mode between 5° and 30°.

Table 2
Isotherms for different adsorbents

	Clay	Activated clay	Modified clay
Freundlich			
q_e (exp) (mgg^{-1})	44.432	37.345	48.265
K_f ($mg\,g^{-1}$)	0.048	0.190	0.467
N	0.491	0.172	0.419
r^2	0.961	0.976	0.963
SD	0.034	0.037	0.006
Langmuir			
K_L ($L\,mmol^{-1}$)	0.011	0.019	1.037
q_m ($mg\,g^{-1}$)	40.385	34.758	46.511
r^2	0.931	0.928	0.998
SD	0.021	0.047	0.007
Temkin			
K_T ($L\,mmol^{-1}$)	0.115	35.535	10.305
r^2	0.973	0.941	0.974
SD	0.017	0.026	0.021
Flory–Huggins			
k_{fh}	1.97×10^{-3}	3.03×10^{-3}	6.98×10^{-3}
n_{fh}	−0.770	−0.738	−0.101
r^2	0.959	0.998	0.973
SD	0.089	0.001	0.006
Halsey			
k_H ($L\,g^{-1}$)	4.420	18.145	5.379
n_H	−0.491	−0.161	−9.895
r^2	0.961	0.982	0.973
SD	0.078	0.114	0.010
DR			
q_m	26.310	24.200	54.686
E_0 ($kJ\,mol^{-1}$)	3.220	0.154	2.690
r^2	0.969	0.994	0.959
SD	0.180	0.065	0.050

2.12. BET surface area measurements

Surface area measurements were analyzed by a surface area analyzer (Micromeritics, ASAP 2020 V3.03H). The specific surface areas were determined from the isotherms using the Brunauer–Emmett–Teller equation.

3. Results and discussion

3.1. IR spectra analysis

The FTIR spectra (Fig. 2) of Mt (C), activated Mt (AC), surfactant modified Mt (MC), and the respective dye-loaded adsorbents (RB21-C), (RB21-AC), and (RB21-MC) are shown in Fig. 2. The shifts in the principal IR frequencies as well as modification of their intensities due to acid treatment and modification with surfactant have proved that there was considerable interaction of H^+ ion/cetyltrimethyl ammonium ions and the clay surface. The band at $797\,cm^{-1}$ (tridymite) has shifted to $800\,cm^{-1}$. The bands at 3,431 and $1{,}636\,cm^{-1}$ for water of hydration showed a significant decrease in AC. The intensities of hydroxyl stretching bands at 3,619 and $3{,}431\,cm^{-1}$ were also reduced in AC, which was due to the removal of octahedral cations causing the loss of water and hydroxyl groups coordinated to them. Furthermore, the new peaks at $3{,}630$–$3{,}655\,cm^{-1}$ in AC were absent in C, which was due to the hydroxyl groups coordinated to Bronsted acid sites in clay [12] and zeolites [29]. In the case of the IR spectrum of RB21-C, the sharp peak at $1{,}560\,cm^{-1}$ is attributed to the aromatic ring vibrations of dye molecules. The aromatic C–H stretching peaks in the range $2{,}924$–$2{,}834\,cm^{-1}$, the C–H in-plane bending peaks of alkyl groups at 1,489 and $1{,}470\,cm^{-1}$ of MC can be attributed to the replacement of interlayer metallic cations by CTAB cations. In addition, the OH stretches at $3{,}600$–$3{,}400\,cm^{-1}$ region, the Si–O stretching peaks between 1,083 and $962\,cm^{-1}$, and the bending peaks within the range 800–$450\,cm^{-1}$ for C were present in the spectrum. Furthermore, the splitting of the methylene scissoring mode at $1{,}489\,cm^{-1}$ was considered to be diagnostic of the packing density increase in the intercalated surfactants within the clay gallery. In the case of the IR spectrum of RB21-MC, the very small peaks in the $1{,}450$–$1{,}400\,cm^{-1}$ region and the feature corresponding to the C = C skeleton stretching at $1{,}560\,cm^{-1}$ were due to aromatic ring vibrations of dye molecules. However, the expected symmetric SO_2 stretching band ($1{,}160$–$1{,}120\,cm^{-1}$) and the asymmetric SO_2 stretching band at $1{,}302\,cm^{-1}$ in the spectra of RB21-C, RB21-AC, and RB21-MC were not seen, which is be probably masked due to overlapping by water and Si–O stretching peaks [30].

3.2. XRD analysis

In the X-ray diffraction pattern of C, AC, and MC (Fig. 3), the main reflections of C were also present in AC but with a slight change in intensity and flex width which implied that only significant amount of clay particles had undergone acid treatment. A diffraction peak at 5.56 Å corresponding to a basal spacing of 15.8 Å, attributed to (001) reflection, was observed in Mt. After modification with CTAB, this peak shifted to a lower angle of 4.6 Å corresponding to a basal spacing of 19.2 Å, suggesting intercalation.

3.3. Thermo gravimetric and BET analysis

Thermogravimetric analysis of C, AC, MC, and CTAB (Fig. 4) indicated that for CTAB complete

Table 3
Kinetic parameters for different adsorbents

	Clay	Activated clay	Modified clay
Pseudo first order			
q_e(exp)	45.003	44.171	44.035
q_e	15.536	9.116	3.433
K_1	0.018	9.05×10^{-3}	4.74×10^{-3}
r^2	0.981	0.949	0.999
SD	0.104	0.101	0.005
Pseudo second order			
q_e	45.766	50.801	59.685
K_2	4.066×10^{-3}	0.0103	0.012
r^2	0.999	0.989	0.977
SD	0.043	0.337	$1.147 \times E^{-4}$
Intraparticle diffusion			
K_{ip}	0.188	0.510	0.268
r^2	0.991	0.979	0.963
SD	0.071	0.168	0.234
Bangham			
K_m	118.871	127.406	119.552
Λ	0.017	0.157	0.031
r^2	0.993	0.985	0.947
SD	$0.627 \times E^{-3}$	0.056	0.027
Liquid film diffusion			
K_{fd}	0.013	0.012	0.008
r^2	0.948	0.979	0.919
SD	0.345	0.168	0.395

q_e (mg/g), K_2 (g/mg min), K_1 (min^{-1}), K_{ip} ($mg/g\,min^{1/2}$), β (g/mg), α (mg/g min).

decomposition took place at ~300°C. However, for MC the loss in mass was only 10% in the temperature range of 280–290°C, suggesting that CTAB molecules were bonded strongly in the interlayer of Mt.

The specific surface area increased slightly in AC (213.968 m^2g^{-1}) as compared to C (209.121 m^2g^{-1}) due to leaching of octahedral ions on acidification. On the other hand in MC, a decrease in specific surface area (150.833 m^2g^{-1}) was observed due to the intercalated CTAB ions clogging up the interlayer space and hindering the access of the nitrogen molecules when measuring the surface area [31].

3.4. Effect of temperature

The dye uptake for C remained constant with increase in temperature (Fig. 5) indicating that the dye uptake onto C was independent of temperature whereas in the case of AC and MC the dye uptake increased with increase in temperature indicating the mechanism to be endothermic. However, the changes observed with AC were less to come to any conclusive evidence. The increase in adsorption with temperature in the case of activated and MC indicated that the mobility of the dye molecules increased with the rising temperature, and increasing temperature produced a swelling effect within the internal structure of the clay enabling large dye molecules to penetrate further [32]. This indicated the mechanism to be chemisorption for AC and MC [33].

3.5. Effect of pH

For C and AC, the maximum adsorption capacity was observed at pH 1.0, which reduced notably as pH was increased to 4.0 and then remained nearly constant (Fig. 5). However, in the case of MC, though maximum adsorption capacity was at pH 1.0, the adsorption remained constant till pH5 and then decreased above pH 5 (~10% decrease). Due to low pKa values of sulfonic acid groups of RB21, the dye could be completely deprotonated at pH 1.0. C exhibited positive zeta potential values at pH1 (13.19 mV while AC exhibited positive zeta potential values at pH 1–2 (7.03,3.69) and highly negative zeta potential values above this pH over the entire range of pH

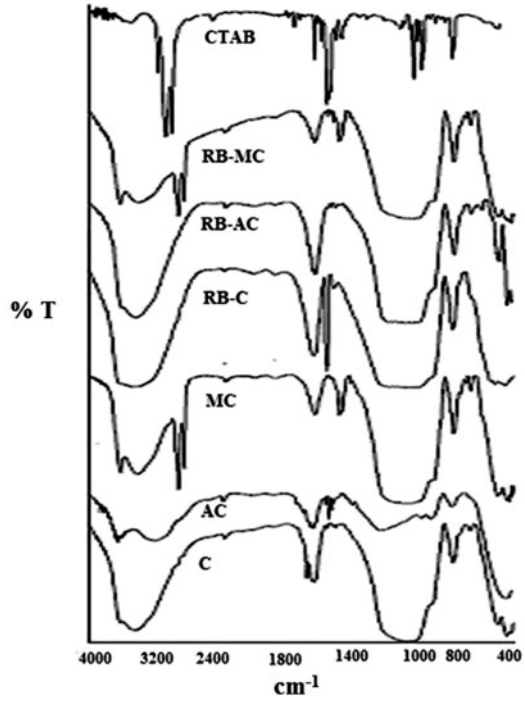

Fig. 2. IR Spectra of adsorbents and dye-loaded adsorbents a) C b) AC c) MC d) RB-C e) RB-AC f) RB-MC g) CTAB.

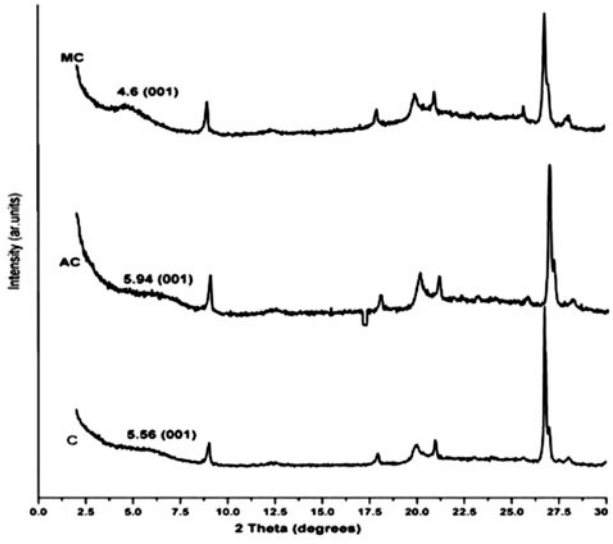

Fig. 3. X-ray diffraction patterns of a) C b) AC c) MC.

studied (Fig. 6). However, the broken edges of clay particles are reported to behave as the metal oxide surface, and these can acquire either positive or negative charge depending on the pH [34]. However, MC exhibited positive zeta potential values over the whole range of pH studied. It exhibited a zeta potential value as high as 49.12 mV at pH 1.0. This implies that adsorption of RB21 onto MC might be due to

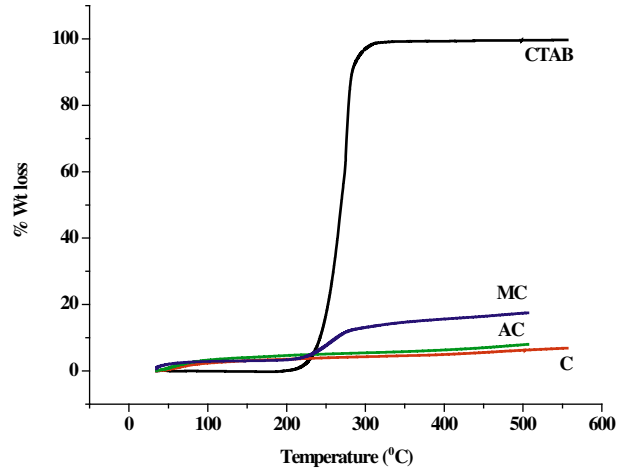

Fig. 4. TGA graphs of a) C, b) AC, c) MC, d) CTAB.

electrostatic attraction between the cationic surfactant head groups in MC, and the dye anions as well as van der Waals interactions between RB21 and the surfactant alkyl chains while its adsorption onto C and AC might be predominantly through electrostatic attractions and ion exchange.

3.6. Effect of adsorbent dose

The adsorption of RB21 increased with increase in adsorbent concentration at low doses and reached saturation limit at 0.2 g for C and 0.8 g for AC and MC (Fig. 5). This trend can be attributed to increased number of adsorbent particles surrounding the adsorbate.

3.7. Effect of concentration of dye

The percent uptake of dye was found to decrease with increase in concentration of dye for all the three adsorbents (Fig. 5), suggesting that limited number of adsorption sites were available for adsorption as concentration of adsorbate molecules increased. However, it is observed that decrease in percent adsorption as concentration increased from 100 to 1000 mg/L was less in the case of AC (~60 to ~50%) and MC (~99 to ~80%) as compared to C (~90 to ~20%). The observed trend in our study for AC and MC could be due to the fact that interaction between dye and adsorbent could have been relatively higher as compared to C [35].

3.8. Sorption isotherm

The isotherm models studied and isotherm constants for the adsorption of RB21 by all the three

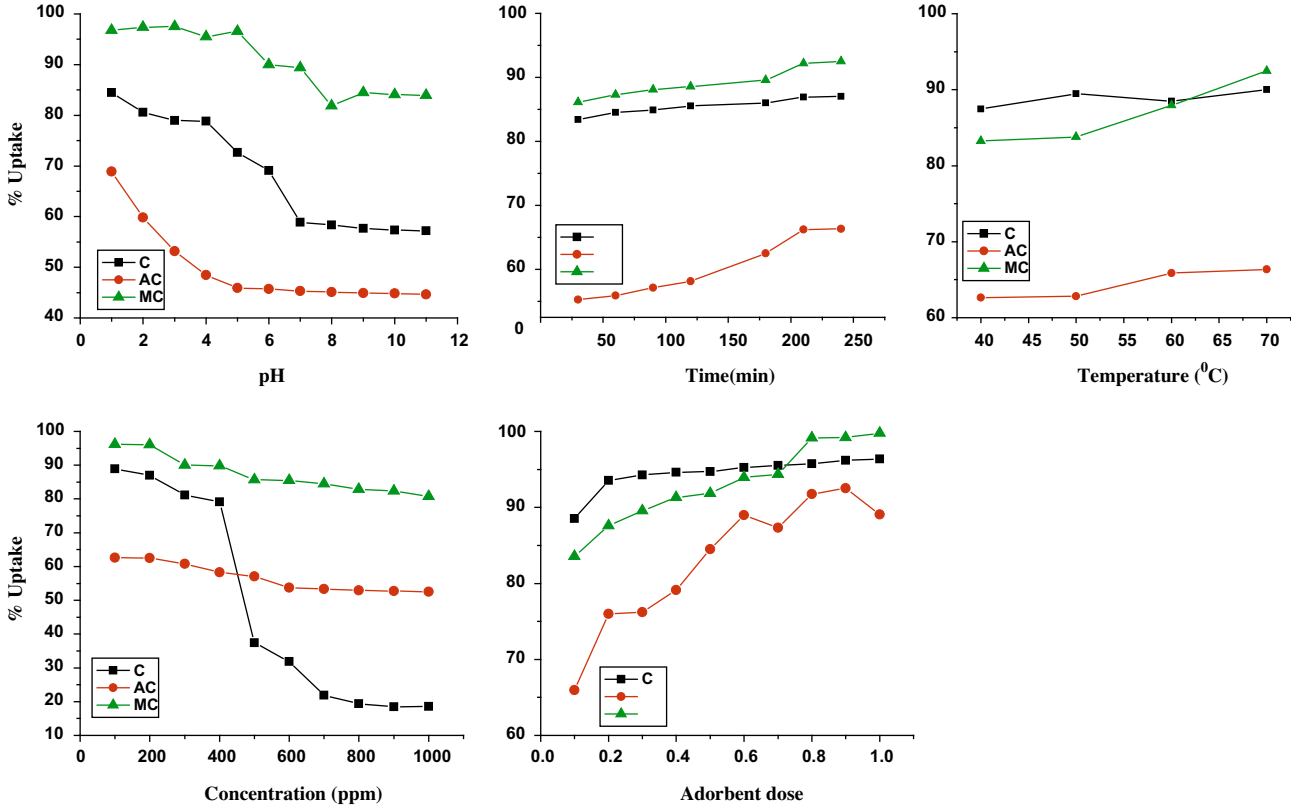

Operating parameters: agitation time -240 min, temperature – 30^{0}C, optimum pH-1, concentration – 100 ppm and adsorbent dose – 0.1 gm

Fig. 5. Effect of (a) pH (1-11) (b) Time (30–240 min) (c) Temperature (40^0—70^0) (d) Concentration (100-1000 ppm) (e) Dose (0.1-1.0 gm).

adsorbents are presented in Table 2. The adsorption data for all the three adsorbents under study for RB21 gave reasonably high correlation coefficient values for all the models studied. Fitting of Langmuir isotherm model suggested the presence of homogeneous adsorption sites. The calculated E values were <8 kJ mol^{-1} for DR model suggesting physisorption for all the three adsorbents under study. The value of Freundlich constant n being less than unity implied that the adsorption intensity was favorable over the entire range of concentrations studied. The fitting of Temkin model indicated favorable adsorption of RB21 onto all the three adsorbents under study. The high regression values for Halsey model suggest multilayer adsorption. Though Flory–Huggins model exhibited high correlation coefficient values, the negative values of n, and low values of k_{FH} imply that the model cannot be used to describe the adsorption data. The q_m values from Langmuir isotherm indicated that MC had higher adsorption capacity (~46 mg/g) as compared to AC

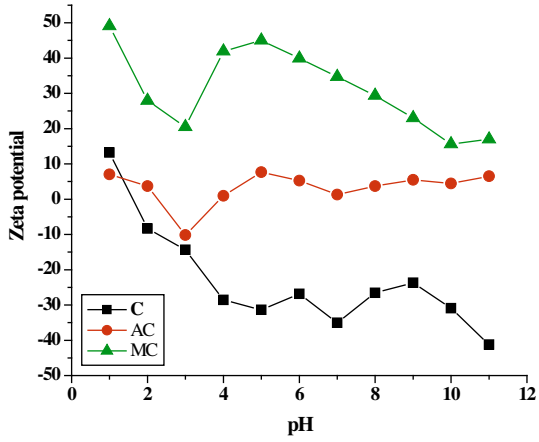

Operating parameters: agitation time -240 min, temperature – 30^{0}C, pH (1-11)

Fig. 6. Zeta potential curves for, (a) C, (b) AC, (c) MC.

(~37 mg/g) and C (~40 mg/g). Comparison of the q_m values obtained from this study and adsorbents was presented in Table 4 [36–42]. It is observed that the

adsorbents have higher adsorption capacity as compared to zeolite and polyurethane foam and lesser adsorption capacity as compared to sepiolite, fly ash, and chitosan. The differences in maximum adsorption capacities of various adsorbents might be due to different adsorption mechanisms of various adsorbents and experimental conditions of adsorption.

3.9. Sorption kinetics

The study of effect of time on the uptake of dye using C, AC, and MC revealed that equilibrium was reached within 90 min for MC and 210 min in the case of C and AC (Fig. 5). The kinetic models were studied and the rate constants for the adsorption of RB21 by all the three adsorbents are presented in Table 3. The correlation coefficients for pseudo-second-order model were found to be greater than the other kinetic models for C, AC, and MC and the calculated equilibrium adsorption capacity values were closer to those obtained experimentally. This supported the assumption behind the model that the surface complexation may be the rate-limiting step involving valence forces through sharing or exchanging of electron between adsorbent and adsorbate. For all the adsorbents under study the plot of q_t versus $t^{1/2}$ did not pass through origin (fig. not shown) suggesting that intraparticle diffusion was not the only rate-controlling step but some degree of the boundary layer diffusion also controlled the adsorption process and that the overall rate of the dye adsorption process appeared to be controlled by more than one step [43,44]. The reasonably good correlation coefficient for Bangham equation indicated that the diffusion of RB21 into the pores of the adsorbents under study also controlled the adsorption process. It was thus concluded that the dye adsorption process was controlled by more than one step.

3.10. Thermodynamic studies

The free energy change values are shown in Table 5. The values of ΔH^0 and ΔS^0 can be calculated from the slope and intercept of the plots of $\ln K_d$ against $1/T$ and are shown in (Table 6). The free energy change during the adsorption process was positive for C and AC suggesting chemisorption to be the predominant mechanism of adsorption while for MC it was negative suggesting the adsorption to be spontaneous. The positive enthalpy change values for AC and MC suggested that the adsorption process was endothermic while for C the enthalpy values were negative. However, the enthalpy change values and the changes in percent adsorption with temperature are too low to come to any conclusion. The negative entropy change corresponded to a decrease in the degree of freedom of the adsorbed species and an orderly adsorption.

3.11. Desorption studies

Desorption studies were done to study the feasibility of reuse of the adsorbents under study. A 0.1 g of adsorbent under study (C, AC, MC) at 25°C was mixed with 25 mL of 100 ppm RB21 solutions maintained at pH1 and agitated for 240 min. The

Table 4
Comparison of adsorption capacity

Adsorbent	Dye	Adsorption Capacity (mg/g)	Reference
Fly ash	Reactive Blue 21	106.71	36
Sepiolite	Reactive Blue 21	66.71	36
Natural zeolite	Reactive Blue 21	9.65	37
Polyurethane foam	Reactive Blue 21	8.31	38
Silylatedpalygorskite	Reactive Blue KER	38	39
Cetyldimethylbenzylammoniumhectorite	Reactive Orange	78	40
Cetylpyridiniumhectorite	Reactive Orange	84	40
Zeolite	Everzol Black, Everzol Red, Everzol Yellow	2.9–7.6	41
Calcinedalunite	Reactive blue 114		
Reactive red 124	170.7	42	
Calcinedalunite	Reactive yellow 64	236	42
Calcinedalunite	Reactive red 124	153	42
Clay	Reactive Blue 21	44.43	This study
Activated clay	Reactive Blue 21	37.34	This study
Modified clay	Reactive Blue 21	48.26	This study

Table 5
Thermodynamic parameters (free energy change) for reactive Blue 21 by clay, activated clay and modified clay

	ΔG (kJ/mol)			
	313 K	323 K	333 K	343 K
Clay	11.735	12.110	12.485	12.860
Activated clay	10.246	10.573	10.900	11.228
Modified clay	−0.096	−0.099	−0.102	−0.106

Table 6
Thermodynamic parameters (Entropy and Enthalpy) for reactive Blue 21 by clay, activated clay and modified clay

	ΔS (J/molK)	ΔH (kJ/mol)	r^2	SD
Clay	−0.037	−0.002	1	0
Activated clay	−0.032	0.010	0.999	0.023
Modified clay	$-6.79 \times E^{-4}$	$3.07 \times E^{-4}$	0.999	$3.87 \times E^{-4}$

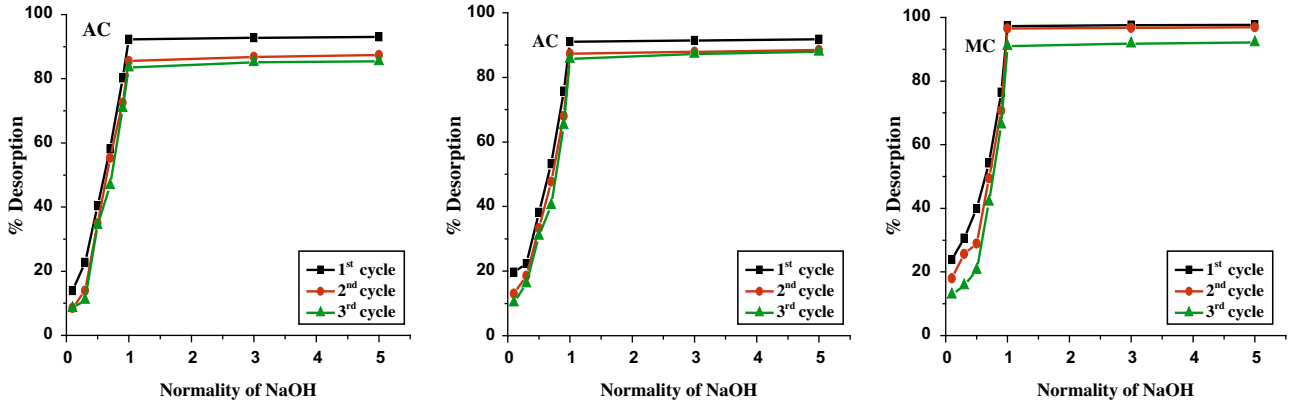

Operating parameters: agitation time -240 min, temperature – 30^0C

Fig. 7. Desorption curves for (a) C, (b) AC, (c) MC.

RB21 loaded adsorbents were filtered, dried, and added into 25 mL of 0.1–5 N NaOH in 100-mL stoppered conical flaks. These flasks were agitated for 240 min. Amount of dye desorbed was determined by use of spectrophotometer. The adsorption–desorption experiments were repeated for 3 cycles. As shown in Fig. 7, the percentage of RB21 desorbed increased with increasing in NaOH concentration. The desorption percentage was 9–23% when 0.1 N NaOH was used and increased to 92–97% when ~1 N NaOH was used for the adsorbents under study. The efficiency of the adsorbent remained almost the same (~5%) for three adsorption–desorption cycles.

4. Conclusions

Montmorillonite (C), acid activated Montmorillonite (AC), and surfactant modified Montmorillonite (MC) were applied to remove Reactive Blue-21 dye from aqueous solution. The intercalation of hexadecyltrimethylammonium ions in Mt increased the basal spacing from 40.49 to 42.03 Å. The study indicated that adsorption process depends upon initial pH, dose of the adsorbent, and contact time. pH 1.0 was found to be optimum for the maximum removal of acid dye onto the adsorbents under study. Among the kinetic models tested, the adsorption kinetics was best described by the pseudo-second-order equation. The data fitted well with Freundlich, Langmuir, Temkin, and Halsey adsorption isotherm models. Adsorption thermodynamics did not give any conclusive evidence for the exothermic or endothermic nature of adsorption mechanism. The adsorbed RB21 could be desorbed efficiently using 1 N NaOH solution, and the adsorbents under study were reusable. Adsorption of RB21 onto MC was attributed to electrostatic attraction

between the cationic surfactant head groups in MC and the dye anions as well as van der Waals interactions between RB21, and the surfactant alkyl chains while its adsorption onto C and AC might be predominantly through electrostatic attractions and ion exchange.

Acknowledgements

This work is supported by University grants commission. The authors thank M.S. University, Vadodara, India, for laboratory facilities. The authors also thank ONGC Vadodara for XRD analysis.

References

[1] D. Mohan, K.P. Singh, G. Singh, K. Kundan, Removal of dyes from wastewater using flyash, a low-cost adsorbent, Ind. Eng. Chem. Res. 41 (2002) 3688–3695.
[2] A. Reife, J.I. Kroschwitz, M. Howe-Grant, M. (Eds.), Kirk–Othmer Encyclopedia of Chemical Technology, Wiley, New York, 8, (1993).
[3] A. Mahwish, Biosorption of reactive dyes. A review, Water Air Soil Pollut. 223 (2012) 2417–2435.
[4] C. Salinas-Hernández, M.C. Díaz-Nava, M. Solache-Ríos, Sorption and desorption of red 5 and yellow 6 by a fe-zeolitic tuff, Water Air Soil Pollut. 223 (2012) 4959–4968.
[5] G.R. Alther, Usingorganoclays to enhance carbon filtration, Waste manage. 22 (2002) 507–513.
[6] J.H. Bae, D.I. Song, J.W. Jeon, Adsorption of anionic dye and surfactant from water onto organomontmorillonite, Sep. Sci. Technol. 35 (2000) 353–365.
[7] J.Q. Jiang, C. Cooper, V. Ouki, Comparison of montmorellonite adsorbents. Part I. preparation, characterization and phenol adsorption, Chemosphere. 47 (2002) 711–716.
[8] R.A. Shawabkeh, M.F. Tutunji, Experimental study and modeling of basic dye sorption by diatomaceous clay, Appl. Clay Sci. 24 (2003) 111–120.
[9] A. Kaya, A.H. Oren, Adsorption of zinc from aqueous solutions to bentonite, J. Hazard. Mater. 125 (2005) 183–189.
[10] D. Karadag, Y. Koc, M. Turan, B. Arumagan, Removal of ammonium ion from aqueous solution using turkish clinoptilolite, J. Hazard. Mater. B136 (2006) 604–609.
[11] J. Smith, S. Bartlett-Hunt, S. Burns, Sorption and permeability of gasoline hydrocarbons in organobentonites porous media, J. Hazard. Mater. B96 (2003) 91–97.
[12] C.T. Cowman, D. White, The mechanism of exchange reactions occurring between sodium montmorillonite and various n-primary amine salts, Trans. of the Faraday Soc. 54 (1958) 691–697.
[13] H.H. Murray, Overview—clay mineral applications, Appl. Clay Sci. 5 (1991) 379–395.
[14] H.H. Murray, Traditional and new applications for kaolin, smectite and palygorskite: a general overview, Appl. Clay Sci. 17 (2000) 207–221.
[15] B.K.G. Theng, D.J. Greenland, J.P. Quirk, Adsorption of alkylammoniumcations by montmorillonite, Clay Minerals. 7 (1967), 1–17.
[16] B.K.G. Theng, The Chemistry of Clay-Organic reactions, Adamlgler, London, (1974), p. 343.
[17] J. Ravichandran, B. Sivasankar, Properties and catalytic activity of acid-modified montmorillonite and vermiculite, Clays Clay Miner. 45 (1997) 854–858.
[18] Z. Li, R.S. Bowman, Sorption of chromate and PCE by surfactant modified clay minerals, Environ. Eng. Sci. 15 (1998) 237–245.
[19] Z. Li, L. Gallus, L. Surface configuration of sorbedhexadecyltrimethylammonium on kaolinite as indicated by surfactant and counterion sorption, cation desorption, and FTIR, Coll and Surf A: Physicochem Eng Aspects. 264 (2005), 61–67.
[20] B.S. Krishna, D.S.R. Murty, D.S.J. Prakash, Thermodynamics of chromium (VI) anionic species sorption onto surfactant-modified montmorillonite clay, J. Colloid. Interf. Sci. 229 (2000) 230–236.
[21] B. Zohra, K. Aicha, S. Fatima, B. Nourredine, B.D. Zoubi, Adsorption of direct red 2 on bentonite modified by cetyltrimethylammonium bromide, J. Chem. Eng. 136 (2008) 295–305.
[22] Z. Li, R.S. Bowman, Retention of inorganic oxyanions by organokaolinite, Water Resour. 35 (2001) 3771–3776.
[23] Z. Li, D. Alessi, P. Zhang, R.S. Bowman, Organo-illite as a low permeability sorbent to retard migration of anionic contaminants, J. Environ. Eng.- ASCE. 128 (2002) 583–587.
[24] Z. Li, C.A. Willms, K. Kniola, Removal of anionic contaminants using surfactant-modified palygorskite and sepiolite, Clays Clay Miner. 51 (2003) 445–451.
[25] Z. Li, Influence of solution pH and ionic strength on chromate uptake by surfactant-modified zeolite, J. Environ. Eng.- ASCE. 130 (2004) 205–208.
[26] A. Ozcan, C. Omeroglu, Y. Erdogan, A.S. Ozcan, Modification of bentonite with a cationic surfactant: an adsorption study of textile dye reactive Blue 19, J. Hazard. Mater. 140 (2007) 173–179.
[27] E.A. Espantaleon, M. Nieto, A. Fernandez, A. Marsal, Use of activated clays in the removal of dyes and surfactants from tannery wastewaters, Appl. Clay Sci. 24 (2003) 105–110.
[28] C. Tanushree, M. Nirendra, Thermal stability of PMMA–clay hybrids, Bull. Mater. Sci. 33 (2010) 165–168.
[29] A. De Stefanis, A.A.G. Toklinson, Towards designing pillared clays for catalysts, Catal. Today 14 (2006) 126–141.
[30] T. Ahmet, B. Nimet, A. Beytullah, E. Mustafa, C. Bulent, E. Erdal, Adsorption of reactive red 120 from aqueous solutions by cethylpyridinium-bentonite, J. Chem. Technol. Biotechnol. 85 (2010) 1199–1207.
[31] R. Malberg, I. Dekany, G. Lagaly, Short-chain alkylammoniummontmorillonites and alcohols: Gas adsorption and immersional wetting, Clay Miner. 24 (1989) 631–647.
[32] B. Acemioglu, Adsorption of congo red from aqueous solution onto calcium-rich fly ash, J. Colloid. Interf. Sci. 274 (2004) 371–379.
[33] W.T. Tsai, Y.M. Chang, C.W. Lai, C.C. Lo, Adsorption of ethyl violet dye in aqueous solution by regenerated spent bleaching earth, J. Colloid. Interf. Sci. 289 (2005) 333–338.
[34] E. Tombacz, M. Szekeres, Colloidal behavior of aqueous montmorillonite suspensions: The specific role of pH in the presence of indifferent electrolytes, Appl. Clay Sci. 27 (2004) 75–94.
[35] T. KantiSen, S. Dawood, Removal of anionic dye Congo red from aqueous solution by raw pine and acid-treated pine cone powder as adsorbent: Equilibrium, thermodynamic, kinetics, mechanism and process design, Water Res. 46 (2012) 1933–1946.
[36] E. Demiras, M.Z. Nas, Batch kinetic and equilibrium studies of adsorption of Reactive Blue 21 by fly ash and sepiolite, Desalination 243 (2009) 8.
[37] S. Tuba, K. Yasemin, K. Selcan, Single and binary adsorption of reactive dyes from aqueous solutions onto clinoptilolite, J. Hazard. Mater. 184 (2010) 164–169.
[38] N. Julieta de Jesus da Silveira, M. Guilherme Costa, S. Carlos Juliano da, R.César, R. EfraimLázaro, Use of Polyurethane foams for the removal of direct red 180 and Reactive Blue 21 dyes in aqueous medium, Desalination 281 (2011) 55.
[39] A. Xue, S. Zhou, Y. Zhao, X. Lu, P. Han, Adsorption of reactive dyes from aqueous solution by silylatedpalygorskite, Appl. Clay Sci. 48 (2010) 638–640.

[40] P. Baskaralingam, M. Pulikesi, V. Ramamurthi, S. Sivanesan, Modified hectorites and adsorption studies of a reactive dye, Appl. Clay Sci. 37 (2007) 207–214.
[41] B. Armagan, M. Turan, M.S. Elik, Equilibrium studies on the adsorption of reactive azo dyes into zeolite, Desalination 170 (2004) 33–39.
[42] M. Ozacar, İ. AyhanŞengil, Adsorption of reactive dyes on calcinedalunite from aqueous solutions, J. Hazard. Mater. 98 (2003) 211–224.
[43] K.G. Bhattacharyya, A. Sharma, Azadirachtaindica leaf powder as an effective biosorbent for dyes: A case study with aqueous Congo red solutions, J. Environ. Manage. 71 (2004) 217–229.
[44] M. Ozacar, I.A. Sengil, Application of kinetic models to the sorption of disperse dyes onto alunite, Colloids Surf. A. 242 (2004) 105–113.